Chapter 8 *Radar Wave Propagation*

In the earlier chapters, radar systems were analyzed with the assumption that the radar waves which traveled to and from targets are in free space. Signal interference due to the earth and its atmosphere was not considered. Despite the fact that *"free space analysis"* may be adequate to provide a general understanding of radar systems, it is only an approximation. In order to accurately predict radar performance, we must modify free space analysis to include the effects of the earth and its atmosphere. This modification should account for ground reflections from the surface of the earth, diffraction of electromagnetic waves, bending or refraction of radar waves due to the earth atmosphere, and attenuation or absorption of radar energy by the gases constituting the atmosphere.

8.1. Earth Atmosphere

The earth atmosphere is compromised of several layers, as illustrated in Fig. 8.1. The first layer which extends in altitude to about 20 Km is known as the troposphere. Electromagnetic waves refract (bend downward) as they travel in the troposphere. The troposphere refractive effect is related to its dielectric constant which is a function of the pressure, temperature, water vapor, and gaseous content. Additionally, due to gases and water vapor in the atmosphere radar energy suffers a loss. This loss is known as the atmospheric attenuation. Atmospheric attenuation increases significantly in the presence of rain, fog, dust, and clouds.

The region above the troposphere (altitude from 20 to 50 Km) behaves like free space, and thus little refraction occurs in this region. This region is known as the interference zone.

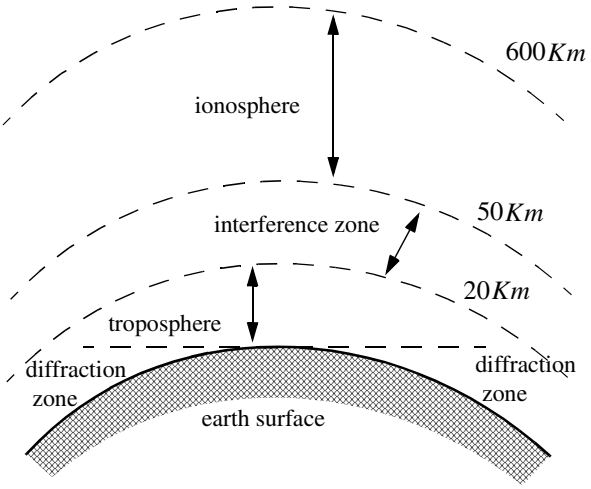

Figure 8.1. Earth atmosphere geometry.

The ionosphere extends from about 50 Km to about 600 Km. It has very low gas density compared to the troposphere. It contains a significant amount of ionized free electrons. The ionization is primarily caused by the sun's ultraviolet and X-rays. This presence of free electrons in the ionosphere affects electromagnetic wave propagation in different ways. These effects include refraction, absorption, noise emission, and polarization rotation. The degree of degradation depends heavily on the frequency of the incident waves. For example, frequencies lower than about 4 to 6 MHz are completely reflected from the lower region of the ionosphere. Frequencies higher than 30 MHz may penetrate the ionosphere with some level of attenuation. In general, as the frequency is increased the ionosphere's effects become less prominent.

The region below the horizon, close to the earth's surface, is called the diffraction region. Diffraction is a term used to describe the bending of radar waves around physical objects. Two types of diffraction are common. They are knife edge and cylinder edge diffraction.

8.2. Refraction

In free space, electromagnetic waves travel in straight lines. However, in the presence of the earth atmosphere, they bend (refract). Refraction is a term used

to describe the deviation of radar wave propagation from straight lines. The deviation from straight line propagation is caused by the variation of the index of refraction. The index of refraction is defined as

$$n = c/v \tag{8.1}$$

where c is the velocity of electromagnetic waves in free space and v is the wave velocity in the medium. Close to the earth's surface the index of refraction is almost unity; however, with increasing altitude the index of refraction decreases gradually. The discussion presented in this chapter assumes a well mixed atmosphere, where the index of refraction decreases in a smooth monotonic fashion with height. The rate of change of the earth's index of refraction n with altitude h is normally referred to as the refractivity gradient, dn/dh. As a result of the negative rate of change in dn/dh, electromagnetic waves travel at slightly higher velocities in the upper troposphere than the lower part. As a result of this, waves traveling horizontally in the troposphere gradually bend downward. In general, since the rate of change in the refractivity index is very slight, waves do not curve downward appreciably unless they travel very long distances through the troposphere.

Refraction affects radar waves in two different ways depending on height. For targets that have altitudes, typically above 100 meters, the effect of refraction is illustrated in Fig. 8.2. In this case, refraction imposes limitations on the radar's capability to measure target position. Refraction introduces an error in measuring the elevation angle.

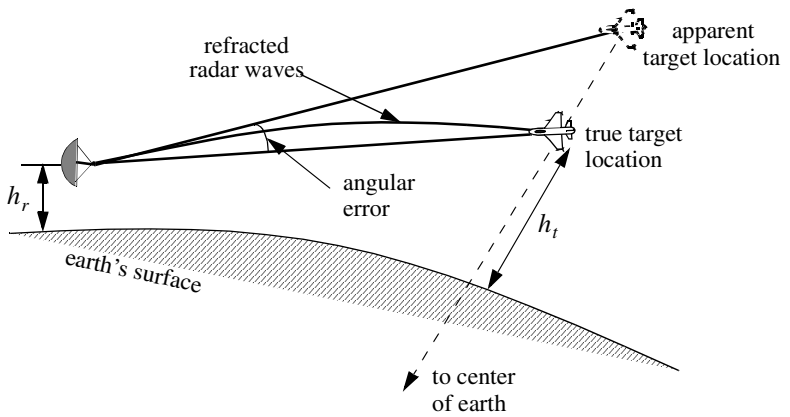

Figure 8.2. Refraction high altitude effect on electromagnetic waves.

In a well mixed atmosphere, the refractivity gradient close to the earth's surface is almost constant. However, temperature changes and humidity lapses close to the earth's surface may cause serious changes in the refractivity profile. When the refractivity index becomes large enough electromagnetic waves bend around the curve of the earth. Consequently, the radar's range to the horizon is extended. This phenomenon is called ducting, and is illustrated in Fig. 8.3. Ducting can be serious over the sea surface, particularly during the hot summertime.

Using ray tracing (geometric optics) an integral-relating range-to-target height with the elevation angle as a parameter can be derived and calculated. However, such computations are complex and numerically intensive. Thus, in practice, radar systems deal with refraction in two different ways, depending on height. For altitudes higher than 3 Km, actual target heights are estimated from look-up tables or from charts of target height versus range for different elevation angles.

Simpler methods that are valid for altitude less than 3 Km, for calculating target height, can also be employed. In this case, the most common way of dealing with refraction is to replace the actual earth with an imaginary earth whose effective radius is $r_e = kr_0$, where r_0 is the actual earth radius, and k is

$$k = \frac{1}{1 + r_0(dn/dh)} \tag{8.2}$$

When the refractivity gradient is assumed to be constant with altitude and is equal to 39×10^{-9} per meter, then $k = 4/3$. Using an effective earth radius $r_e = (4/3)r_0$ produces what is known as the *"four third earth model."* In general, choosing

$$r_e = r_0(1 + 6.37 \times 10^{-3}(dn/dh)) \tag{8.3}$$

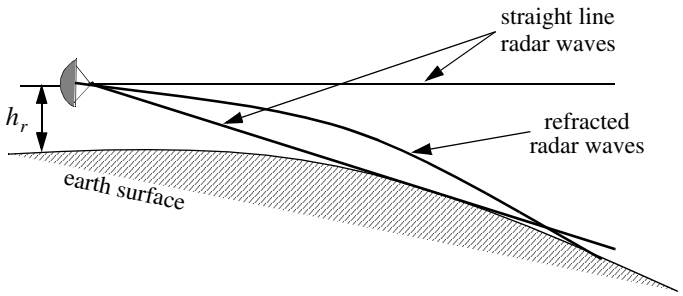

Figure 8.3. Refraction low altitude effect on electromagnetic waves.

produces a propagation model where waves travel in straight lines. Selecting the correct value for k depends heavily on the region's meteorological conditions. Blake[1] derives the *"height-finding equation"* for the 4/3 earth. It is

$$h = h_r + 6076R\sin\theta + 0.6625R^2(\cos\theta)^2 \tag{8.4}$$

where h and h_r are in feet and R is nautical miles. All variables are defined in Fig. 8.4.

The distance to the horizon for a radar located at height h_r can be calculated with the help of Fig. 8.5. For the right-angle triangle OBA we get

$$r_h = \sqrt{(r_0 + h_r)^2 - r_0^2} \tag{8.5}$$

where r_h is the distance to the horizon. By expanding Eq. (8.5) and collecting terms we can derive the expression for the distance to the horizon as

$$r_h^2 = 2r_0h_r + h_r^2 \tag{8.6}$$

Finally, since $r_0 \gg h_r$ Eq. (8.6) is approximated by

$$r_h \approx \sqrt{2r_0h_r} \tag{8.7}$$

and when refraction is accounted for, Eq. (8.7) becomes

$$r_h \approx \sqrt{2r_eh_r} \tag{8.8}$$

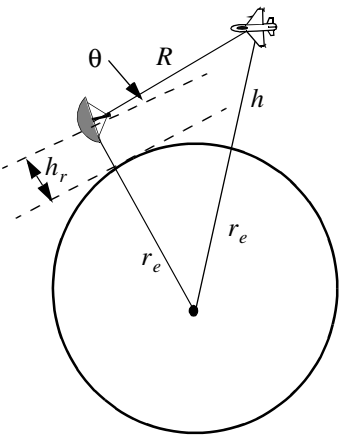

Figure 8.4. Measuring target height for 4/3 earth.

1. Blake, L. V., *Radar Range-Performance Analysis*, Artech House, 1986.

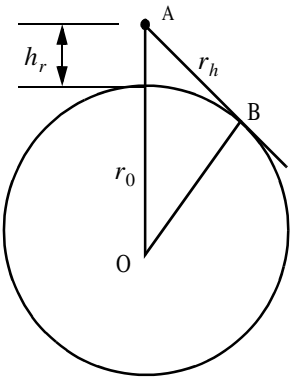

Figure 8.5. Measuring the distance to the horizon.

8.3. Ground Reflection

When radar waves are reflected from the earth's surface, they suffer a loss in amplitude and a change in phase. Three factors that contribute to these changes that are the overall ground reflection coefficient are the reflection coefficient for a flat surface, the divergence factor due to earth curvature, and the surface roughness.

8.3.1. Smooth Surface Reflection Coefficient

The smooth surface reflection coefficient depends on the frequency, on the surface dielectric coefficient, and on the radar grazing angle. The vertical polarization and the horizontal polarization reflection coefficients are

$$\Gamma_v = \frac{\varepsilon \sin\psi_g - \sqrt{\varepsilon - (\cos\psi_g)^2}}{\varepsilon \sin\psi_g + \sqrt{\varepsilon - (\cos\psi_g)^2}} \tag{8.9}$$

$$\Gamma_h = \frac{\sin\psi_g - \sqrt{\varepsilon - (\cos\psi_g)^2}}{\sin\psi_g + \sqrt{\varepsilon - (\cos\psi_g)^2}} \tag{8.10}$$

where ψ_g is the grazing angle (incident angle) and ε is the complex dielectric constant of the surface, and are given by

$$\varepsilon = \varepsilon' - j\varepsilon'' \tag{8.11}$$

Typical values of ε' and ε" can be found tabulated in the literature. For example, seawater at $28°C$ has ε' = 65 and ε" = 30.7 at X-band. Fig. 8.6 shows the corresponding magnitude plots for Γ_h and Γ_v, while Fig. 8.7 shows the phase plots. The plots shown in those figures show the general typical behavior of the reflection coefficient.

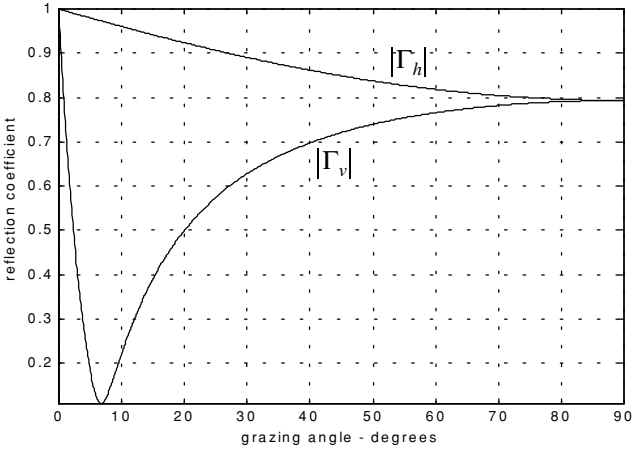

Figure 8.6. Reflection coefficient magnitude.

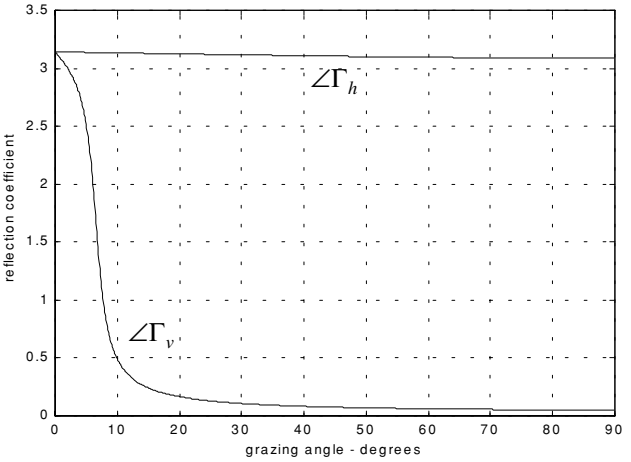

Figure 8.7. Reflection coefficient phase.

Note that when $\psi_g = 90°$ we get

$$\Gamma_h = \frac{1-\sqrt{\varepsilon}}{1+\sqrt{\varepsilon}} = -\frac{\varepsilon-\sqrt{\varepsilon}}{\varepsilon+\sqrt{\varepsilon}} = -\Gamma_v \tag{8.12}$$

while when the grazing angle is very small ($\psi_g \approx 0$), we have

$$\Gamma_h = -1 = \Gamma_v \tag{8.13}$$

Observation of Figs. 8.6 and 8.7 yield the following conclusions: (1) The magnitude of the reflection coefficient with horizontal polarization is equal to unity at very small grazing angles and it decreases monotonically as the angle is increased. (2) The magnitude of the vertical polarization has a well defined minimum. The angle that corresponds to this condition is called Brewster's polarization angle. For this reason, airborne radars in the look-down mode utilize mainly vertical polarization to significantly reduce the terrain bounce reflections. (3) For horizontal polarization the phase is almost π; however, for vertical polarization the phase changes to zero around the Brewster's angle. (4) For very small angles (less than $2°$) both $|\Gamma_h|$ and $|\Gamma_v|$ are nearly one; $\angle\Gamma_h$ and $\angle\Gamma_v$ are nearly π. Thus, little difference in the propagation of horizontally or vertically polarized waves exists at low grazing angles.

MATLAB Function "ref_coef.m"

The function *"ref_coef.m"* calculates and plots the horizontal and vertical magnitude and phase response of the reflection coefficient. It is given in Section 8.7. The syntax is as follows

[rh,rv,ph,pv] = ref_coef (epsp,epspp)

where

Symbol	Description	Status
epsp	ε'	*input*
epspp	ε''	*input*
rh	*vector of* $\|\Gamma_h\|$	*output*
rv	*vector of* $\|\Gamma_v\|$	*output*
ph	*vector of* $\angle\Gamma_h$	*output*
vh	*vector of* $\angle\Gamma_v$	*output*

8.3.2. Divergence

The overall reflection coefficient is also affected by the round earth divergence factor, D. When an electromagnetic wave is incident on a round earth surface, the reflected wave diverges because of the earth's curvature. This is illustrated in Fig. 8.8a. Due to divergence the reflected energy is defocused, and the radar power density is reduced. The divergence factor can be derived using geometrical considerations. A widely accepted approximation for the divergence factor is given by

$$D \approx \frac{1}{\sqrt{1 + \dfrac{2r_1 r_2}{r_e r \sin\psi_g}}} \tag{8.14}$$

where all variables in Eq. (8.14) are defined in Fig. 8.8b.

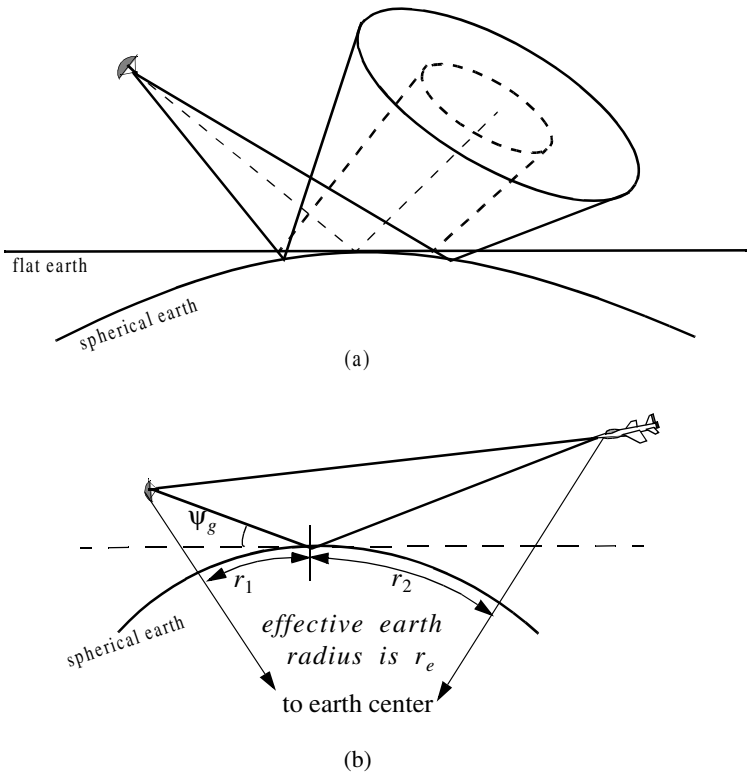

Figure 8.8. Illustration of divergence. (a) Solid line: Ray perimeter for spherical earth. Dashed line: Ray perimeter for flat earth. (b) Definition of variables in Eq. (8.14)

8.3.3. Rough Surface Reflection

In addition to divergence, surface roughness also affects the reflection coefficient. Surface roughness is given by

$$S_r = e^{-2\left(\frac{2\pi h_{rms}\sin\psi_g}{\lambda}\right)^2} \tag{8.15}$$

where h_{rms} is the rms surface height irregularity. In general, rays reflected from rough surfaces undergo changes in phase and amplitude, which results in the diffused (non-coherent) portion of the reflected signal. Combining the above three factors, we can express the total reflection coefficient Γ_t as

$$\Gamma_t = \Gamma_{(h,v)} D S_r \tag{8.16}$$

$\Gamma_{(h,v)}$ is the horizontal or vertical smoothed surface reflection coefficient.

8.4. The Pattern Propagation Factor

In general, the pattern propagation factor is a term used to describe the wave propagation when free space conditions are not met. This factor is defined separately for the transmitting and receiving paths. The propagation factor also accounts for the radar antenna pattern effects. The basic definition of the propagation factor is

$$F = \left|E/E_0\right| \tag{8.17}$$

where E is the electric field in the medium and E_0 is the free space electric field.

Near the surface of the earth, multipath propagation effects dominate the formation of the propagation factor. In this section, a general expression for the propagation factor due to multipath will be developed. In this sense, the propagation factor describes the constructive/destructive interference of the electromagnetic waves diffracted from the earth surface (which can be either flat or curved). The subsequent sections derive the specific forms of the propagation factor due to flat and curved earth.

Consider the geometry shown in Fig. 8.9. The radar is located at height h_r. The target is at range R, and is located at a height h_t. The grazing angle is ψ_g. The radar energy emanating from its antenna will reach the target via two paths: the "direct path" AB and the "indirect path" ACB. The lengths of the paths AB and ACB are normally very close to one another and thus, the difference between the two paths is very small. Denote the direct path as R_d, the indirect path as R_i, and the difference as $\Delta R = R_i - R_d$. It follows that the phase difference between the two paths is given by

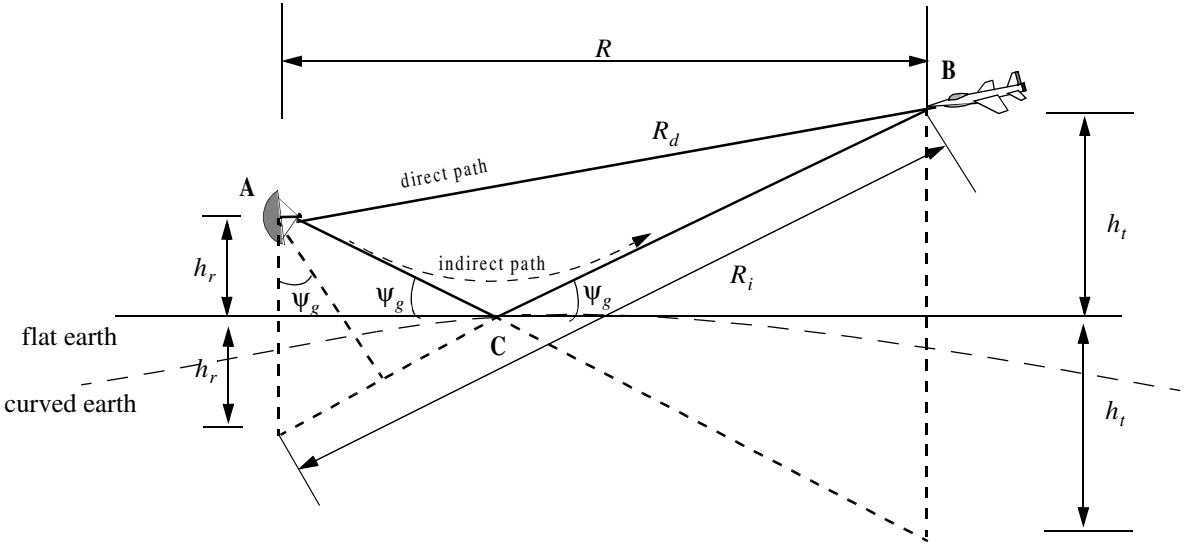

Figure 8.9. Geometry for multipath propagation.

$$\Delta\Phi = \frac{2\pi}{\lambda}\Delta R \tag{8.18}$$

where λ is the radar wavelength.

The indirect signal amplitude arriving at the target is less than the signal amplitude arriving via the direct path. This is because the antenna gain in the direction of the indirect path is less than that along the direct path, and because the signal reflected from the earth surface at point C is modified in amplitude and phase in accordance to the earth's reflection coefficient, Γ. The earth reflection coefficient is given by

$$\Gamma = \rho e^{j\varphi} \tag{8.19}$$

where ρ is less than unity and φ describes the phase shift induced on the indirect path signal due to surface roughness.

The direct signal (in volts) arriving at the target via the direct path can be written as

$$E_d = e^{j\omega_0 t} e^{j\frac{2\pi}{\lambda}R_d} \tag{8.20}$$

where the time harmonic term $\exp(j\omega_0 t)$ represents the signal's time dependency, and the exponential term $\exp(j(2\pi/\lambda)R_d)$ represents the signal spatial phase. The indirect signal at the target is

$$E_i = \rho e^{j\varphi} e^{j\omega_0 t} e^{j\frac{2\pi}{\lambda}R_i} \tag{8.21}$$

where $\rho\exp(j\varphi)$ is the surface reflection coefficient. Therefore, the overall signal arriving at the target is

$$E = E_d + E_i = e^{j\omega_0 t} e^{j\frac{2\pi}{\lambda}R_d}\left(1 + \rho e^{j\left(\varphi + \frac{2\pi}{\lambda}(R_i - R_d)\right)}\right) \tag{8.22}$$

Due to reflections from the earth surface, the overall signal strength is then modified at the target by the ratio of the signal strength in the presence of earth to the signal strength at the target in free space. From Eq. (8.17) the modulus of this ratio is the propagation factor. By using Eqs. (8.20) and (8.22) the propagation factor is computed as

$$F = \left|\frac{E_d}{E_d + E_i}\right| = \left|1 + \rho e^{j\varphi} e^{j\Delta\Phi}\right| \tag{8.23}$$

which can be rewritten as

$$F = \left|1 + \rho e^{j\alpha}\right| \tag{8.24}$$

where $\alpha = \Delta\Phi + \varphi$. Using Euler's identity ($e^{j\alpha} = \cos\alpha + j\sin\alpha$), Eq. (8.24) can be written as

$$F = \sqrt{1 + \rho^2 + 2\rho\cos\alpha} \tag{8.25}$$

It follows that the signal power at the target is modified by the factor F^2. By using reciprocity, the signal power at the radar is computed by multiplying the radar equation by the factor F^4. In the following two sections we will develop exact expressions for the propagation factor for flat and curved earth.

The propagation factor for free space and no multipath is $F = 1$. Denote the radar detection range in free space (i.e., $F = 1$) as R_0. It follows that the detection range in the presence of the atmosphere and multipath interference is

$$R = \frac{R_0 F}{(L_a)^{1/4}} \tag{8.26}$$

where L_a is the two-way atmospheric loss at range R. Atmospheric attenuation will be discussed in a later section. Thus, for the purpose of illustrating the effect of multipath interference on the propagation factor, assume that $L_a = 1$. In this case, Eq. (8.26) is modified to

$$R = R_0 F \tag{8.27}$$

Fig. 8.10 shows the general effects of multipath interference on the propagation factor. Note that, due to the presence of surface reflections, the antenna elevation coverage is transformed into a lobed pattern structure. The lobe widths are directly proportional to λ, and inversely proportional to h_r. A target located at a maxima will be detected at twice its free space range. Alternatively, at other angles, the detection range will be less than that in free space.

8.4.1. Flat Earth

Using the geometry of Fig. 8.9, the direct and indirect paths are computed as

$$R_d = \sqrt{R^2 + (h_t - h_r)^2} \tag{8.28}$$

$$R_i = \sqrt{R^2 + (h_t + h_r)^2} \tag{8.29}$$

Eqs. (8.28) and (8.29) can be approximated using the truncated binomial series expansion as

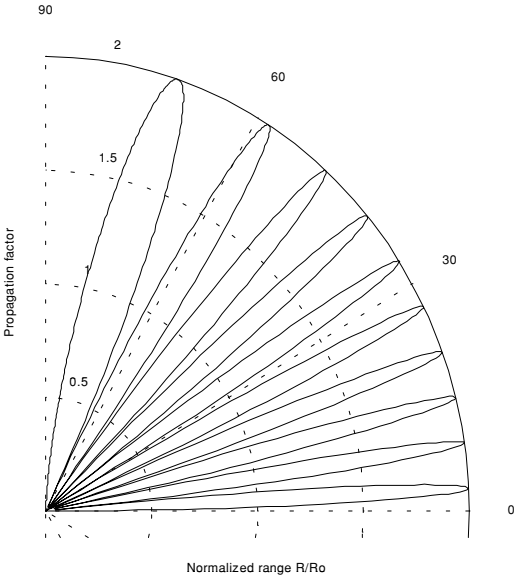

Figure 8.10. Vertical lobe structure due to the reflecting surface as a function of the elevation angle.

$$R_d \approx R + \frac{(h_t - h_r)^2}{2R} \tag{8.30}$$

$$R_i \approx R + \frac{(h_t + h_r)^2}{2R} \tag{8.31}$$

This approximation is valid for low grazing angles, where $R \gg h_t, h_r$. It follows that

$$\Delta R = R_i - R_d \approx \frac{2h_t h_r}{R} \tag{8.32}$$

Substituting Eq. (8.32) into Eq. (8.18) yields the phase difference due to multipath propagation between the two signals (direct and indirect) arriving at the target. More precisely,

$$\Delta\Phi = \frac{2\pi}{\lambda}\Delta R \approx \frac{4\pi h_t h_r}{\lambda R} \tag{8.33}$$

At this point assume smooth surface with reflection coefficient $\Gamma = -1$. This assumption means that waves reflected from the surface suffer no amplitude loss, and that the induced surface phase shift is equal to 180°. Using Eq. (8.18) and Eq. (8.25) along with these assumptions yield

$$F^2 = 2 - 2\cos\Delta\Phi = 4(\sin(\Delta\Phi/2))^2 \tag{8.34}$$

Substituting Eq. (8.33) into Eq. (8.34) yields

$$F^2 = 4\left(\sin\frac{2\pi h_t h_r}{\lambda R}\right)^2 \tag{8.35}$$

By using reciprocity, the expression for the propagation factor at the radar is then given by

$$F^4 = 16\left(\sin\frac{2\pi h_t h_r}{\lambda R}\right)^4 \tag{8.36}$$

Finally, the signal power at the radar is computed by multiplying the radar equation by the factor F^4,

$$P_r = \frac{P_t G^2 \lambda^2 \sigma}{(4\pi)^3 R^4} \; 16\left(\sin\frac{2\pi h_t h_r}{\lambda R}\right)^4 \tag{8.37}$$

Since the sine function varies between 0 and 1, the signal power will then vary between 0 and 16. Therefore, the fourth power relation between signal power and the target range results in varying the target range from 0 to twice the actual range in free space. In addition to that, the field strength at the radar will now have holes that correspond to the nulls of the propagation factor.

The nulls of the propagation factor occur when the sine is equal to zero. More precisely,

$$\frac{2h_r h_t}{\lambda R} = n \tag{8.38}$$

where $n = \{0, 1, 2, \ldots\}$. The maxima occur at

$$\frac{4h_r h_t}{\lambda R} = n + 1 \tag{8.39}$$

The target heights that produce nulls in the propagation factor are $\{h_t = n(\lambda R/2h_r); n = 0, 1, 2, \ldots\}$, and the peaks are produced from target heights $\{h_t = n(\lambda R/4h_r); n = 1, 2, \ldots\}$. Therefore, due to the presence of surface reflections, the antenna elevation coverage is transformed into a lobed pattern structure as illustrated by Fig. 8.10. A target located at a maxima will be detected at twice its free space range. Alternatively, at other angles, the

detection range will be less than that in free space. At angles defined by Eq. (8.38) there would be no measurable target returns.

For small angles, Eq. (8.37) can be approximated by

$$P_r \approx \frac{4\pi P_t G^2 \sigma}{\lambda^2 R^8} (h_t h_r)^4 \tag{8.40}$$

Thus, the received signal power varies as the eighth power of the range instead of the fourth power. Also, the factor $G\lambda$ is now replaced by G/λ.

8.4.2. Spherical Earth

In order to model the effects of multipath propagation on radar performance more accurately, we need to remove the flat earth condition and account for the earth's curvature. When considering round earth, electromagnetic waves travel in curved paths because of the atmospheric refraction. And as mentioned earlier, the most commonly used approach to mitigating the effects of atmospheric refraction is to replace the actual earth by an imaginary earth such that electromagnetic waves travel in straight lines. The effective radius of the imaginary earth is

$$r_e = kr_0 \tag{8.41}$$

where k is a constant and r_0 is the actual earth radius ($6371 Km$). Using the geometry in Fig. 8.11, the direct and indirect path difference is

$$\Delta R = R_1 + R_2 - R_d \tag{8.42}$$

The propagation factor is computed by using ΔR from Eq. (8.42) in Eq. (8.18) and substituting the result in Eq. (8.25). To compute (R_1, R_2, and R_d) the following cubic equation must first be solved for r_1:

$$2r_1^3 - 3rr_1^2 + (r^2 - 2r_e(h_r + h_t))r_1 + 2r_e h_r r = 0 \tag{8.43}$$

The solution is

$$r_1 = \frac{r}{2} - p\sin\frac{\xi}{3} \tag{8.44}$$

where

$$p = \frac{2}{\sqrt{3}}\sqrt{r_e(h_t + h_r) + \frac{r^2}{4}} \tag{8.45}$$

$$\xi = \operatorname{asin}\left(\frac{2r_e r(h_t - h_r)}{p^3}\right) \tag{8.46}$$

Next, we solve for R_1, R_2, and R_d. From Fig. 8.11,

$$\phi_1 = r_1 / r_e \tag{8.47}$$

$$\phi_2 = r_2 / r_e \tag{8.48}$$

Using the law of cosines to the triangles ABO and BOC yields

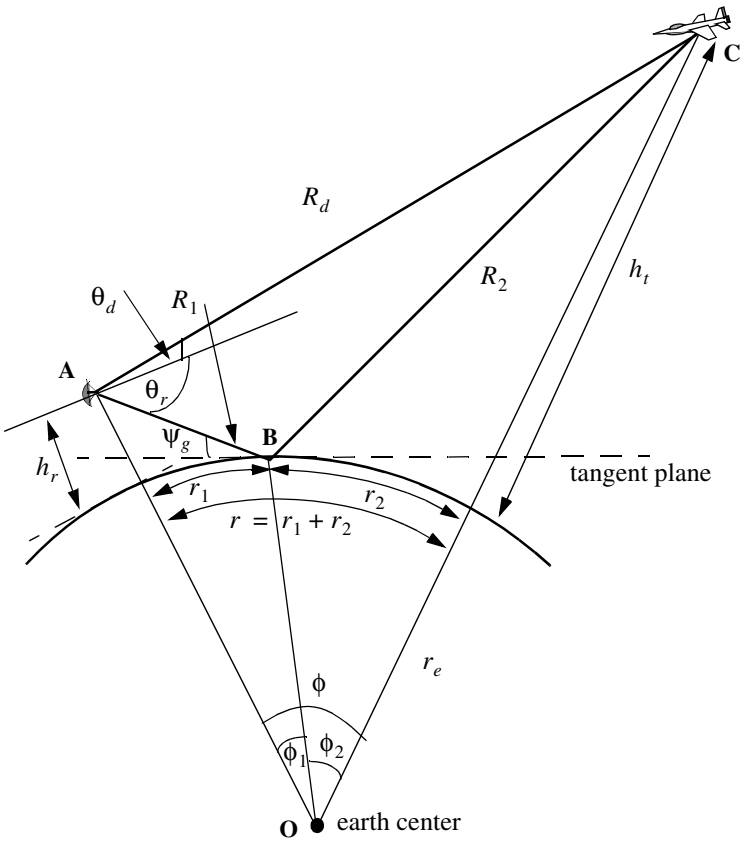

Figure 8.11. Geometry associated with multipath propagation over round earth.

$$R_1 = \sqrt{r_e^2 + (r_e + h_r)^2 - 2r_e(r_e + h_r)\cos\phi_1} \tag{8.49}$$

$$R_2 = \sqrt{r_e^2 + (r_e + h_t)^2 - 2r_e(r_e + h_t)\cos\phi_2} \tag{8.50}$$

Eqs. (8.49) and (8.50) can be written in the following simpler forms:

$$R_1 = \sqrt{h_r^2 + 4r_e(r_e + h_r)(\sin(\phi_1/2))^2} \tag{8.51}$$

$$R_2 = \sqrt{h_t^2 + 4r_e(r_e + h_t)(\sin(\phi_2/2))^2} \tag{8.52}$$

Using the law of cosines on the triangle AOC yields

$$R_d = \sqrt{(h_t - h_r)^2 + 4(r_e + h_t)(r_e + h_r)\left(\sin\left(\frac{\phi_1 + \phi_2}{2}\right)\right)^2} \tag{8.53}$$

Substituting Eqs. (8.51) through (8.53) directly into Eq. (8.42) may not be conducive to numerical accuracy. A more suitable form for the computation of ΔR is then derived. The detailed derivation is in Blake. The results are listed below. For better numerical accuracy use the following expression to compute ΔR:

$$\Delta R = \frac{4R_1R_2(\sin\psi_g)^2}{R_1 + R_2 + R_d} \tag{8.54}$$

where

$$\psi_g \approx \operatorname{asin}\left(\frac{h_t}{R_1} - \frac{R_1}{2r_e}\right) \tag{8.55}$$

8.5. Diffraction

Diffraction is a term used to describe the phenomenon of electromagnetic waves bending around obstacles. It is of major importance to radar systems operating at very low altitudes. Hills and ridges diffract radio energy and make it possible to perform detection in regions that are physically shadowed. In practice, experimental data measurements provide the dominant source of information available on this phenomenon. Some theoretical analyses of diffraction are also available. However, in these cases many assumptions are made, and perhaps the most important assumption is that obstacles are chosen to be perfect conductors.

The problem of propagation over a knife edge on a plane can be described with help of Fig. 8.12. The target and radar heights are denoted, respectively,

by h_t and h_r. The edge height is h_e. Denote the distance by which the radar rays clear (or do not clear) the tip of the edge by δ. As a matter of notation δ is assumed to be positive when the direct rays clear the edge, and is negative otherwise. Because of the fact that ground reflection occurs on both sides of the edge, then the propagation factor is composed of four distinct rays, as illustrated in Fig. 8.13. An expression for the propagation factor corresponding to the four rays is reported in Meeks (see Bibliography).

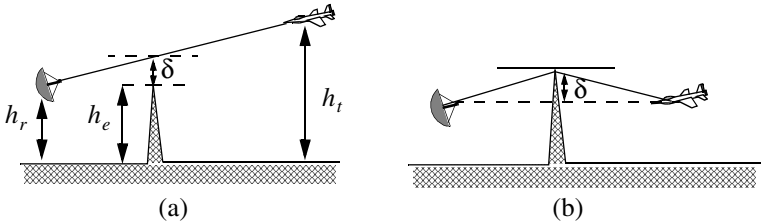

Figure 8.12. Diffraction over a knife edge. (a) Positive δ. (b) Negative δ.

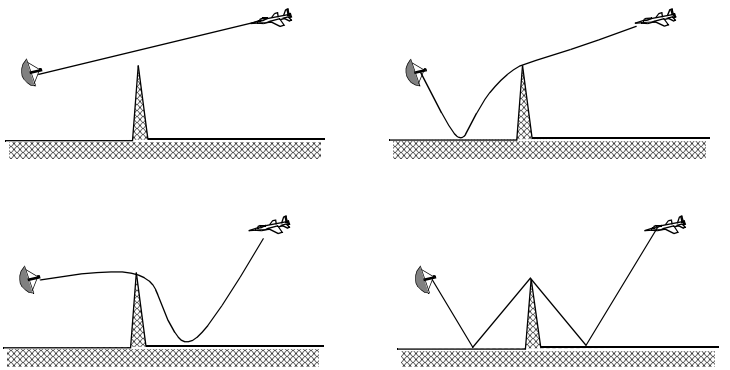

Figure 8.13. Four ray formation.

8.6. Atmospheric Attenuation

Electromagnetic waves travel in free space without suffering any energy loss. Alternatively, due to gases and water vapor in the atmosphere radar

energy suffers a loss. This loss is known as the atmospheric attenuation. Atmospheric attenuation increases significantly in the presence of rain, fog, dust, and clouds. Most of the lost radar energy is normally absorbed by gases and water vapor and transformed into heat, while a small portion of this lost energy is used in molecular transformation of the atmosphere particles.

The two-way atmospheric attenuation over a range R can be expressed as

$$L_{atmosphere} = e^{-2\alpha R} \tag{8.56}$$

where α is the one-way attenuation coefficient. Water vapor attenuation peaks at about $22.3 GHz$, while attenuation due to oxygen peaks at between 60 and $118 GHz$. Atmospheric attenuation is severe for frequencies higher than $35 GHz$. This is the reason why ground-based radars rarely use frequencies higher than $35 GHz$.

Atmospheric attenuation is a function range, frequency, and elevation angle. Fig. 8.14 shows a typical two-way atmospheric attenuation plot versus range at $3 GHz$, with the elevation angle as a parameter. Fig. 8.15 is similar to Fig. 8.14, except it is for $10 GHz$. For further details on this subject the reader is advised to visit Blake.

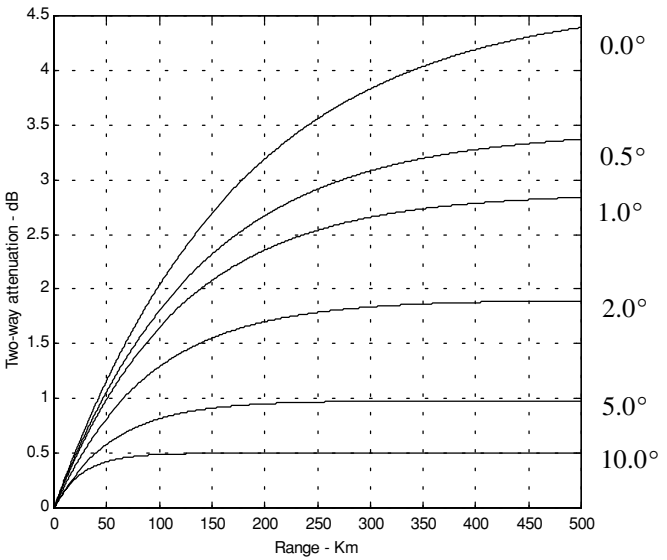

Figure 8.14. Attenuation versus range; frequency is *3 GHz*.

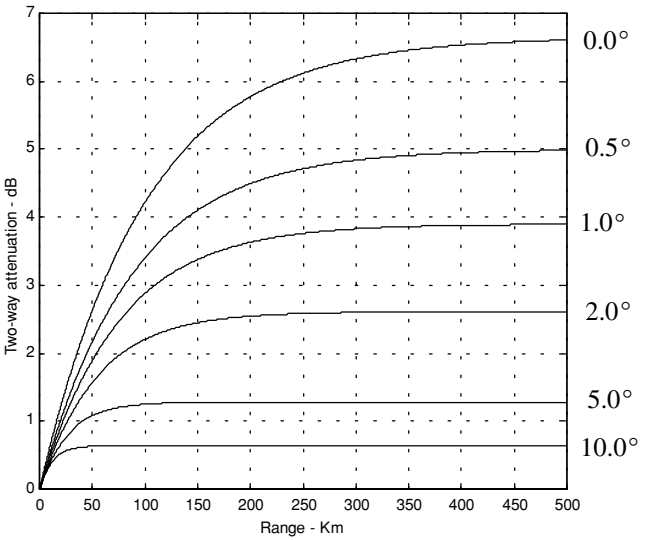

Figure 8.15. Attenuation versus range; frequency is *10 GHz.*

8.7. MATLAB Program "ref_coef.m"

```
function [rh,rv,ph,pv] = ref_coef (epsp,epspp)
eps = epsp - i * epspp; %65.0-30.7i;
psi = 0:0.1:90;
psirad = psi.*(pi/180.);
arg1 = eps-(cos(psirad).^2);
arg2 = sqrt(arg1);
arg3 = sin(psirad);
arg4 = eps.*arg3;
rv = (arg4-arg2)./(arg4+arg2);
rh = (arg3-arg2)./(arg3+arg2);
gamamodv = abs(rv);
gamamodh = abs(rh);
figure(1)
plot(psi,gamamodv,'k',psi,gamamodh,'k -.');
axis tight
grid
xlabel('grazing angle - degrees');
ylabel('reflection coefficient - amplitude')
```

```
legend ('Vertical Polarization','Horizontal Polarization')
pv = -angle(rv);
ph = angle(rh);
figure(2)
plot(psi,pv,'k',psi,ph,'k -.');
grid
xlabel('grazing angle - degrees');
ylabel('reflection coefficient - phase')
legend ('Vertical Polarization','Horizontal Polarization')
```

Problems

8.1. Using Eq. (8.4), determine h when $h_r = 15m$ and $R = 35Km$.

8.2. An exponential expression for the index of refraction is given by

$$n = 1 + 315 \times 10^{-6} \exp(-0.136h)$$

where the altitude h is in Km. Calculate the index of refraction for a well mixed atmosphere at 10% and 50% of the troposphere.

8.3. Rederive Eq. (8.34) assuming vertical polarization.

8.4. Reproduce Figs. 8.6 and 8.7 by using $f = 8GHz$ and (a) $\varepsilon' = 2.8$ and $\varepsilon'' = 0.032$ (dry soil); (b) $\varepsilon' = 47$ and $\varepsilon'' = 19$ (sea water at $0°C$); (c) $\varepsilon' = 50.3$ and $\varepsilon'' = 18$ (lake water at $0°C$).

8.5. In reference to Fig. 8.9, assume a radar height of $h_r = 100m$ and a target height of $h_t = 500m$. The range is $R = 20Km$. (a) Calculate the lengths of the direct and indirect paths. (b) Calculate how long it will take a pulse to reach the target via the direct and indirect paths.

8.6. In the previous problem, assuming that you may be able to use the small grazing angle approximation: (a) Calculate the ratio of the direct to the indirect signal strengths at the target. (b) If the target is closing on the radar with velocity $v = 300m/s$, calculate the Doppler shift along the direct and indirect paths. Assume $\lambda = 3cm$.

8.7. Utilizing the plots generated in solving Problem 8.4, derive an emperical expression for the Brewster's angle.

8.8. A radar at altitude $h_r = 10m$ and a target at altitude $h_t = 300m$, and assuming a spherical earth, calculate r_1, r_2, and ψ_g.

8.9. Derive an asymptotic form for Γ_h and Γ_v when the grazing angle is very small.

8.10. In reference to Fig. 8.8, assume a radar height of $h_r = 100m$ and a target height of $h_t = 500m$. The range is $R = 20Km$. (a) Calculate the lengths of the direct and indirect paths. (b) Calculate how long it will take a pulse to reach the target via the direct and indirect paths.

8.11. Using the law of cosines, derive Eqs. (8.51) through (8.53).

8.12. In the previous problem, assuming that you may be able to use the small grazing angle approximation: (a) Calculate the ratio of the direct to the indirect signal strengths at the target. (b) If the target is closing on the radar with velocity $v = 300m/s$, calculate the Doppler shift along the direct and indirect paths. Assume $\lambda = 3cm$.

8.13. In the previous problem, assuming that you may be able to use the small grazing angle approximation: (a) Calculate the ratio of the direct to the indirect signal strengths at the target. (b) If the target is closing on the radar with velocity $v = 300m/s$, calculate the Doppler shift along the direct and indirect paths. Assume $\lambda = 3cm$.

8.14. Calculate the range to the horizon corresponding to a radar at $5Km$ and $10Km$ of altitude. Assume 4/3 earth.

8.15. Develop a mathematical expression that can be used to reproduce Figs. 8.14 and 8.15.